

Search for a Technicolor ω_T Particle in Events with a Photon and a b -quark Jet at CDF

F. Abe,¹⁷ H. Akimoto,³⁹ A. Akopian,³¹ M. G. Albrow,⁷ A. Amadon,⁵ S. R. Amendolia,²⁷ D. Amidei,²⁰ J. Antos,³³
S. Aota,³⁷ G. Apollinari,³¹ T. Arisawa,³⁹ T. Asakawa,³⁷ W. Ashmanskas,⁵ M. Atac,⁷ P. Azzi-Bacchetta,²⁵
N. Bacchetta,²⁵ S. Bagdasarov,³¹ M. W. Bailey,²² P. de Barbaro,³⁰ A. Barbaro-Galtieri,¹⁸ V. E. Barnes,²⁹
B. A. Barnett,¹⁵ M. Barone,⁹ G. Bauer,¹⁹ T. Baumann,¹¹ F. Bedeschi,²⁷ S. Behrends,³ S. Belforte,²⁷ G. Bellettini,²⁷
J. Bellinger,⁴⁰ D. Benjamin,³⁵ J. Bensinger,³ A. Beretvas,⁷ J. P. Berge,⁷ J. Berryhill,⁵ S. Bertolucci,⁹ S. Bettelli,²⁷
B. Bevensee,²⁶ A. Bhatti,³¹ K. Biery,⁷ C. Bigongiari,²⁷ M. Binkley,⁷ D. Bisello,²⁵ R. E. Blair,¹ C. Blocker,³
K. Bloom,²⁰ S. Blusk,³⁰ A. Bodek,³⁰ W. Bokhari,²⁶ G. Bolla,²⁹ Y. Bonushkin,⁴ D. Bortoletto,²⁹ J. Boudreau,²⁸
L. Breccia,² C. Bromberg,²¹ N. Bruner,²² R. Brunetti,² E. Buckley-Geer,⁷ H. S. Budd,³⁰ K. Burkett,¹¹ G. Busetto,²⁵
A. Byon-Wagner,⁷ K. L. Byrum,¹ M. Campbell,²⁰ A. Caner,²⁷ W. Carithers,¹⁸ D. Carlsmith,⁴⁰ J. Cassada,³⁰
A. Castro,²⁵ D. Cauz,³⁶ A. Cerri,²⁷ P. S. Chang,³³ P. T. Chang,³³ H. Y. Chao,³³ J. Chapman,²⁰ M. -T. Cheng,³³
M. Chertok,³⁴ G. Chiarelli,²⁷ C. N. Chiou,³³ F. Chlebana,⁷ L. Christofek,¹³ R. Cropp,¹⁴ M. L. Chu,³³ S. Cihangir,⁷
A. G. Clark,¹⁰ M. Cobal,²⁷ E. Cocca,²⁷ M. Contreras,⁵ J. Conway,³² J. Cooper,⁷ M. Cordelli,⁹ D. Costanzo,²⁷
C. Couyoumtzelis,¹⁰ D. Cronin-Hennessy,⁶ R. Culbertson,⁵ D. Dagenhart,³⁸ T. Daniels,¹⁹ F. DeJongh,⁷
S. Dell'Agnello,⁹ M. Dell'Orso,²⁷ R. Demina,⁷ L. Demortier,³¹ M. Deninno,² P. F. Derwent,⁷ T. Devlin,³²
J. R. Dittmann,⁶ S. Donati,²⁷ J. Done,³⁴ T. Dorigo,²⁵ N. Eddy,¹³ K. Einsweiler,¹⁸ J. E. Elias,⁷ R. Ely,¹⁸
E. Engels, Jr.,²⁸ W. Erdmann,⁷ D. Errede,¹³ S. Errede,¹³ Q. Fan,³⁰ R. G. Feild,⁴¹ Z. Feng,¹⁵ C. Ferretti,²⁷ I. Fiori,²
B. Flaughner,⁷ G. W. Foster,⁷ M. Franklin,¹¹ J. Freeman,⁷ J. Friedman,¹⁹ H. Frisch,⁵ Y. Fukui,¹⁷ S. Gadomski,¹⁴
S. Galeotti,²⁷ M. Gallinaro,²⁶ O. Ganel,³⁵ M. Garcia-Sciveres,¹⁸ A. F. Garfinkel,²⁹ C. Gay,⁴¹ S. Geer,⁷
D. W. Gerdes,²⁰ P. Giannetti,²⁷ N. Giokaris,³¹ P. Giromini,⁹ G. Giusti,²⁷ M. Gold,²² A. Gordon,¹¹ A. T. Goshaw,⁶
Y. Gotra,²⁸ K. Goulianos,³¹ H. Grassmann,³⁶ C. Green,²⁹ L. Groer,³² C. Grosso-Pilcher,⁵ G. Guillian,²⁰
J. Guimaraes da Costa,¹⁵ R. S. Guo,³³ C. Haber,¹⁸ E. Hafen,¹⁹ S. R. Hahn,⁷ R. Hamilton,¹¹ T. Handa,¹²
R. Handler,⁴⁰ W. Hao,³⁵ F. Happacher,⁹ K. Hara,³⁷ A. D. Hardman,²⁹ R. M. Harris,⁷ F. Hartmann,¹⁶ J. Hauser,⁴
E. Hayashi,³⁷ J. Heinrich,²⁶ A. Heiss,¹⁶ B. Hinrichsen,¹⁴ K. D. Hoffman,²⁹ C. Holck,²⁶ R. Hollebeek,²⁶
L. Holloway,¹³ Z. Huang,²⁰ B. T. Huffman,²⁸ R. Hughes,²³ J. Huston,²¹ J. Huth,¹¹ H. Ikeda,³⁷ M. Incagli,²⁷
J. Incandela,⁷ G. Introzzi,²⁷ J. Iwai,³⁹ Y. Iwata,¹² E. James,²⁰ H. Jensen,⁷ U. Joshi,⁷ E. Kajfasz,²⁵ H. Kambara,¹⁰
T. Kamon,³⁴ T. Kaneko,³⁷ K. Karr,³⁸ H. Kasha,⁴¹ Y. Kato,²⁴ T. A. Keaffaber,²⁹ K. Kelley,¹⁹ R. D. Kennedy,⁷
R. Kephart,⁷ D. Kestenbaum,¹¹ D. Khazins,⁶ T. Kikuchi,³⁷ B. J. Kim,²⁷ H. S. Kim,¹⁴ S. H. Kim,³⁷ Y. K. Kim,¹⁸
L. Kirsch,³ S. Klimentenko,⁸ D. Knoblauch,¹⁶ P. Koehn,²³ A. Königter,¹⁶ K. Kondo,³⁷ J. Konigsberg,⁸ K. Kordas,¹⁴
A. Korytov,⁸ E. Kovacs,¹ W. Kowald,⁶ J. Kroll,²⁶ M. Kruse,³⁰ S. E. Kuhlmann,¹ E. Kuns,³² K. Kurino,¹²
T. Kuwabara,³⁷ A. T. Laasanen,²⁹ S. Lami,²⁷ S. Lammell,⁷ J. I. Lamoureux,³ M. Lancaster,¹⁸ M. Lanzoni,²⁷
G. Latino,²⁷ T. LeCompte,¹ S. Leone,²⁷ J. D. Lewis,⁷ M. Lindgren,⁴ T. M. Liss,¹³ J. B. Liu,³⁰ Y. C. Liu,³³
N. Lockyer,²⁶ O. Long,²⁶ M. Loreti,²⁵ D. Lucchesi,²⁷ P. Lukens,⁷ S. Lusin,⁴⁰ J. Lys,¹⁸ K. Maeshima,⁷
P. Maksimovic,¹¹ M. Mangano,²⁷ M. Mariotti,²⁵ J. P. Marriner,⁷ G. Martignon,²⁵ A. Martin,⁴¹ J. A. J. Matthews,²²
P. Mazzanti,² K. McFarland,³⁰ P. McIntyre,³⁴ P. Melese,³¹ M. Menguzzato,²⁵ A. Menzione,²⁷ E. Meschi,²⁷
S. Metzler,²⁶ C. Miao,²⁰ T. Miao,⁷ G. Michail,¹¹ R. Miller,²¹ H. Minato,³⁷ S. Miscetti,⁹ M. Mishina,¹⁷
S. Miyashita,³⁷ N. Moggi,²⁷ E. Moore,²² Y. Morita,¹⁷ A. Mukherjee,⁷ T. Muller,¹⁶ A. Munar,²⁷ P. Murat,²⁷
S. Murgia,²¹ M. Musy,³⁶ H. Nakada,³⁷ T. Nakaya,⁵ I. Nakano,¹² C. Nelson,⁷ D. Neuberger,¹⁶ C. Newman-Holmes,⁷
C.-Y. P. Ngan,¹⁹ L. Nodulman,¹ A. Nomerotski,⁸ S. H. Oh,⁶ T. Ohmoto,¹² T. Ohsugi,¹² R. Oishi,³⁷ M. Okabe,³⁷
T. Okusawa,²⁴ J. Olsen,⁴⁰ C. Pagliarone,²⁷ R. Paoletti,²⁷ V. Papadimitriou,³⁵ S. P. Pappas,⁴¹ N. Parashar,²⁷
A. Parri,⁹ J. Patrick,⁷ G. Pauletta,³⁶ M. Paulini,¹⁸ A. Perazzo,²⁷ L. Pescara,²⁵ M. D. Peters,¹⁸ T. J. Phillips,⁶
G. Piacentino,²⁷ M. Pillai,³⁰ K. T. Pitts,⁷ R. Plunkett,⁷ A. Pompos,²⁹ L. Pondrom,⁴⁰ J. Proudfoot,¹ F. Ptohos,¹¹
G. Punzi,²⁷ K. Ragan,¹⁴ D. Reher,¹⁸ M. Reischl,¹⁶ A. Ribon,²⁵ F. Rimondi,² L. Ristori,²⁷ W. J. Robertson,⁶
A. Robinson,¹⁴ T. Rodrigo,²⁷ S. Rolli,³⁸ L. Rosenson,¹⁹ R. Roser,¹³ T. Saab,¹⁴ W. K. Sakumoto,³⁰ D. Saltzberg,⁴
A. Sansoni,⁹ L. Santi,³⁶ H. Sato,³⁷ P. Schlabach,⁷ E. E. Schmidt,⁷ M. P. Schmidt,⁴¹ A. Scott,⁴ A. Scribano,²⁷
S. Segler,⁷ S. Seidel,²² Y. Seiya,³⁷ F. Semeria,² T. Shah,¹⁹ M. D. Shapiro,¹⁸ N. M. Shaw,²⁹ P. F. Shepard,²⁸
T. Shibayama,³⁷ M. Shimojima,³⁷ M. Shochet,⁵ J. Siegrist,¹⁸ A. Sill,³⁵ P. Sinervo,¹⁴ P. Singh,¹³ K. Sliwa,³⁸
C. Smith,¹⁵ F. D. Snider,¹⁵ J. Spalding,⁷ T. Speer,¹⁰ P. Sphicas,¹⁹ F. Spinella,²⁷ M. Spiropulu,¹¹ L. Spiegel,⁷
L. Stanco,²⁵ J. Steele,⁴⁰ A. Stefanini,²⁷ R. Ströhmer,^{7a} J. Strologas,¹³ F. Strumia,¹⁰ D. Stuart,⁷ K. Sumorok,¹⁹
J. Suzuki,³⁷ T. Suzuki,³⁷ T. Takahashi,²⁴ T. Takano,²⁴ R. Takashima,¹² K. Takikawa,³⁷ M. Tanaka,³⁷
B. Tannenbaum,⁴ F. Tartarelli,²⁷ W. Taylor,¹⁴ M. Tecchio,²⁰ P. K. Teng,³³ Y. Teramoto,²⁴ K. Terashi,³⁷ S. Tether,¹⁹
D. Theriot,⁷ T. L. Thomas,²² R. Thurman-Keup,¹ M. Timko,³⁸ P. Tipton,³⁰ A. Titov,³¹ S. Tkaczyk,⁷ D. Toback,⁵
K. Tollefson,³⁰ A. Tollestrup,⁷ H. Toyoda,²⁴ W. Trischuk,¹⁴ J. F. de Troconiz,¹¹ S. Truitt,²⁰ J. Tseng,¹⁹ N. Turini,²⁷

T. Uchida,³⁷ F. Ukegawa,²⁶ J. Valls,³² S. C. van den Brink,¹⁵ S. Vejcik, III,²⁰ G. Velev,²⁷ I. Volobouev,¹⁸ R. Vidal,⁷ R. Vilar,^{7a} D. Vucinic,¹⁹ R. G. Wagner,¹ R. L. Wagner,⁷ J. Wahl,⁵ N. B. Wallace,²⁷ A. M. Walsh,³² C. Wang,⁶ C. H. Wang,³³ M. J. Wang,³³ A. Warburton,¹⁴ T. Watanabe,³⁷ T. Watts,³² R. Webb,³⁴ C. Wei,⁶ H. Wenzel,¹⁶ W. C. Wester, III,⁷ A. B. Wicklund,¹ E. Wicklund,⁷ R. Wilkinson,²⁶ H. H. Williams,²⁶ P. Wilson,⁷ B. L. Winer,²³ D. Winn,²⁰ D. Wolinski,²⁰ J. Wolinski,²¹ S. Worm,²² X. Wu,¹⁰ J. Wyss,²⁷ A. Yagil,⁷ W. Yao,¹⁸ K. Yasuoka,³⁷ G. P. Yeh,⁷ P. Yeh,³³ J. Yoh,⁷ C. Yosef,²¹ T. Yoshida,²⁴ I. Yu,⁷ A. Zanetti,³⁶ F. Zetti,²⁷ and S. Zucchelli²

(CDF Collaboration)

- ¹ Argonne National Laboratory, Argonne, Illinois 60439
- ² Istituto Nazionale di Fisica Nucleare, University of Bologna, I-40127 Bologna, Italy
- ³ Brandeis University, Waltham, Massachusetts 02254
- ⁴ University of California at Los Angeles, Los Angeles, California 90024
- ⁵ University of Chicago, Chicago, Illinois 60637
- ⁶ Duke University, Durham, North Carolina 27708
- ⁷ Fermi National Accelerator Laboratory, Batavia, Illinois 60510
- ⁸ University of Florida, Gainesville, Florida 32611
- ⁹ Laboratori Nazionali di Frascati, Istituto Nazionale di Fisica Nucleare, I-00044 Frascati, Italy
- ¹⁰ University of Geneva, CH-1211 Geneva 4, Switzerland
- ¹¹ Harvard University, Cambridge, Massachusetts 02138
- ¹² Hiroshima University, Higashi-Hiroshima 724, Japan
- ¹³ University of Illinois, Urbana, Illinois 61801
- ¹⁴ Institute of Particle Physics, McGill University, Montreal H3A 2T8, and University of Toronto, Toronto M5S 1A7, Canada
- ¹⁵ The Johns Hopkins University, Baltimore, Maryland 21218
- ¹⁶ Institut für Experimentelle Kernphysik, Universität Karlsruhe, 76128 Karlsruhe, Germany
- ¹⁷ National Laboratory for High Energy Physics (KEK), Tsukuba, Ibaraki 305, Japan
- ¹⁸ Ernest Orlando Lawrence Berkeley National Laboratory, Berkeley, California 94720
- ¹⁹ Massachusetts Institute of Technology, Cambridge, Massachusetts 02139
- ²⁰ University of Michigan, Ann Arbor, Michigan 48109
- ²¹ Michigan State University, East Lansing, Michigan 48824
- ²² University of New Mexico, Albuquerque, New Mexico 87131
- ²³ The Ohio State University, Columbus, Ohio 43210
- ²⁴ Osaka City University, Osaka 588, Japan
- ²⁵ Università di Padova, Istituto Nazionale di Fisica Nucleare, Sezione di Padova, I-35131 Padova, Italy
- ²⁶ University of Pennsylvania, Philadelphia, Pennsylvania 19104
- ²⁷ Istituto Nazionale di Fisica Nucleare, University and Scuola Normale Superiore of Pisa, I-56100 Pisa, Italy
- ²⁸ University of Pittsburgh, Pittsburgh, Pennsylvania 15260
- ²⁹ Purdue University, West Lafayette, Indiana 47907
- ³⁰ University of Rochester, Rochester, New York 14627
- ³¹ Rockefeller University, New York, New York 10021
- ³² Rutgers University, Piscataway, New Jersey 08855
- ³³ Academia Sinica, Taipei, Taiwan 11530, Republic of China
- ³⁴ Texas A&M University, College Station, Texas 77843
- ³⁵ Texas Tech University, Lubbock, Texas 79409
- ³⁶ Istituto Nazionale di Fisica Nucleare, University of Trieste/ Udine, Italy
- ³⁷ University of Tsukuba, Tsukuba, Ibaraki 305, Japan
- ³⁸ Tufts University, Medford, Massachusetts 02155
- ³⁹ Waseda University, Tokyo 169, Japan
- ⁴⁰ University of Wisconsin, Madison, Wisconsin 53706
- ⁴¹ Yale University, New Haven, Connecticut 06520

If the Technicolor ω_T particle exists, a likely decay mode is $\omega_T \rightarrow \gamma\pi_T$, followed by $\pi_T \rightarrow b\bar{b}$, yielding the signature $\gamma b\bar{b}$. We have searched 85 pb⁻¹ of data collected by the CDF experiment at

the Fermilab Tevatron for events with a photon and two jets, where one of the jets must contain a secondary vertex implying the presence of a b quark. We find no excess of events above standard model expectations. We express the result as an exclusion region in the $M_{\omega_T} - M_{\pi_T}$ mass plane.

PACS numbers 13.85Rm, 13.85Qk, 14.80.-j

In the standard model of electroweak interactions, the elementary scalar fields of the Higgs mechanism break electroweak symmetry and give mass to the W and Z gauge bosons. A new particle is predicted, the Higgs boson, which couples to quarks and leptons, and causes the fermions to acquire mass. Technicolor is a dynamical version of the Higgs mechanism which does not contain elementary scalar bosons [1]. In this approach, there are new heavy fermions interacting via the new, strong technicolor gauge interaction. These technifermions form vacuum condensates that perform the mass-generating functions of elementary scalars. They also form new boson bound states, including the $\pi_T^{0,\pm}$, $\rho_T^{0,\pm}$ and ω_T , analogous to the mesons of QCD.

In $p\bar{p}$ collisions a quark and an anti-quark may annihilate into a virtual photon which can fluctuate into a particle with the same quantum numbers, such as the hypothetical ω_T . In the model of Technicolor considered here [2], the ω_T may decay to $\gamma\pi_T$ followed by the decay $\pi_T \rightarrow b\bar{b}$; the resulting signature is $\gamma b\bar{b}$. We have searched for events with a photon, a b quark jet and at least one additional jet, in 85 pb^{-1} of $p\bar{p}$ collisions at $\sqrt{s} = 1.8 \text{ TeV}$ collected by the CDF experiment in 1994-1995. In this Letter we describe the search and the resulting limits on ω_T and π_T mass combinations.

We briefly describe the relevant aspects of the CDF detector [3]. A superconducting solenoidal magnet provides a 1.4 T magnetic field in a volume 3 m in diameter and 5 m long, containing three tracking devices. Closest to the beamline is a 4-layer silicon microstrip detector (SVX) [4] used to identify the secondary vertices from b -hadron decays. Outside the SVX, a time projection chamber locates the z position of the interaction. In the region with radius from 30 cm to 132 cm is the central tracking chamber (CTC) which measures charged-particle momenta. Surrounding the magnet coil is the electromagnetic calorimeter which is in turn surrounded by the hadronic calorimeter. The calorimeters are constructed of towers, subtending 15° in ϕ and 0.1 in η , pointing to the interaction region. In the central region ($|\eta| < 1.1$), on the inner face of the calorimeter, is the central preradiator wire chamber (CPR). This device is used to determine if a photon began its shower in the magnet coil. At a depth of six radiation lengths into the electromagnetic calorimeter, wire chambers with cathode strip readout (central electromagnetic strip chamber, CES) measure two orthogonal profiles of showers.

Collisions producing a photon candidate are selected by a three-level trigger which requires a central electromagnetic cluster with $E_T > 23 \text{ GeV}$ and limited additional energy in the region of the calorimeter surrounding the cluster. Offline, we select events with an electromagnetic cluster with $E_T > 25 \text{ GeV}$ and $|\eta| < 1.0$. Electron and jet backgrounds are reduced by requiring the cluster to be isolated from additional energy in the calorimeter, other energy deposits in the CES, and charged-particle

tracks in the CTC. These requirements yield a data sample of 511,335 events.

Photon backgrounds, dominated by jets that fragment to an energetic $\pi^0 \rightarrow \gamma\gamma$ and are misidentified as a single photon, are measured using the shower shape in the CES system for photon $E_T < 35$ GeV and the probability of a conversion before the CPR for $E_T > 35$ GeV [5]. We find $55 \pm 1 \pm 15\%$ of these photon candidates are actually jets misidentified as photons.

Jets in the events are clustered with a cone of 0.4 in $\eta-\phi$ space. The jet energies are corrected for calorimeter gaps and non-linear response, energy not contained in the jet cone and underlying event energy [6]. We then select events with at least two jets, each with $E_T > 30$ GeV and $|\eta| < 2.0$. This reduces the data set to 10,182 events.

One of the jets is required to be identified as a b -quark jet by the algorithm used in the top-quark analysis [7]. This algorithm searches for tracks in the SVX that are associated with the jet but not associated with the primary vertex, indicating they come from the decay of a long-lived particle. We require that the track, extrapolated to the interaction vertex, has a distance of closest approach greater than 2.5 times its uncertainty. At least two of these tracks must form a vertex that is displaced from the interaction vertex. The tag's decay length, L_{xy} , is defined in the transverse plane as the dot product of the vector pointing from the primary vertex to the secondary vertex and a unit vector along the jet axis. We require $|L_{xy}|/\sigma > 3$. These requirements constitute a "tag". In the data sample the tag is required to be positive, with $L_{xy} > 0$. This final selection reduces the data set to 200 events.

A sample of multi-jet events is used to study the backgrounds to the tags [8]. For each jet in this sample, the E_T of the jet, the number of SVX tracks associated with the jet, and the scalar sum of the E_T in the event are recorded. The probability of tagging the jet is determined as a function of these variables for negative tags, with $L_{xy} < 0$. Negative tags occur due to measurement resolution and errors in reconstruction. Since these effects should produce negative and positive tags with equal probability, the negative tagging probability can be used as the probability of finding a positive tag due to mismeasurement (mistags).

To estimate the standard model background to the 200-event data sample, we sum three sources: events with jets misidentified as photons, events with photons and mistags and events with standard model production of photons with heavy flavor quarks. Using the photon background method described above, the number of events with a jet misidentified as a photon is $56 \pm 30 \pm 8$ events [9]. The large statistical uncertainty is due to the low discrimination power of the method, and the systematic uncertainty reflects the uncertainty in the background composition and the level of internal consistency in the method. It is necessary to directly measure the

jets misidentified as photons in this tagged sample, rather than apply a universal photon background fraction, since the production of photons in events with specific quark content will have different production cross sections, due to the quark charges and masses, and therefore different ratios to the jet backgrounds.

To estimate the number of real photons and mistags, we apply the photon background method and the negative tagging probability to the data sample before the tagging requirement. The estimate of this background is $27 \pm 5 \pm 14$ events. The 50% systematic uncertainty accommodates a discrepancy in the number of predicted and observed negative tags (312 and 197, respectively) in a sample of events with a photon and one jet. This discrepancy may be caused by the difference in the QCD control sample, where two jets opposite each other cause hadronization with a balanced set of tracks to locate the primary vertex, and the photon sample, which does not have the same balanced tracking topology. The final source of backgrounds, standard model production of a photon with a heavy quark, is estimated using a custom Monte Carlo [10]. We expect $25 \pm 2 \pm 13$ events from $\gamma b\bar{b}$ production and $23 \pm 3 \pm 12$ events from $\gamma c\bar{c}$ production. The systematic uncertainty includes a conservative estimate of the uncertainty in the leading-order calculation. The total background estimate is $131 \pm 30 \pm 29$ events, and correlations between uncertainties have been included. We conclude that the 200 events in the data sample do not constitute a significant excess over standard model expectations.

To set limits on the Technicolor model [2], we investigate points in the $M_{\omega_T} - M_{\pi_T}$ mass plane on a 20 GeV/c² grid. We also investigate a baseline point at $M_{\omega_T} = 210$ GeV/c² and $M_{\pi_T} = 110$ GeV/c², suggested by the authors of the model. At each point in the grid, limits are set using the following procedure. Two invariant masses are calculated for each event: the mass of the tagged jet and the highest- E_T untagged jet, M_{jj} , corresponding to the π_T mass, and the mass of the two jets plus the photon, $M_{jj\gamma}$, corresponding to the ω_T mass. The distributions of M_{jj} and $M_{jj\gamma} - M_{jj}$ for the data are shown in Figure 1. We collect the events with M_{jj} within a window around M_{π_T} , $|M_{jj} - M_{\pi_T}| < 0.36M_{\pi_T}$, which is selected to be 90% efficient for the signal. For these events, we histogram the mass difference $\Delta M = M_{jj\gamma} - M_{jj}$ where a signal would appear as a peak. The mass difference has good resolution since the poor jet resolution is largely canceled. We fit the ΔM spectrum above 50 GeV/c² to a background distribution and a Gaussian peak. The central value of the Gaussian is fixed to the ΔM of the grid point and the width is fixed to the expected value, $\sqrt{\Delta M/(4 \text{ GeV}/c^2)}$ GeV/c², which is the experimental resolution. (The Technicolor particles have negligible natural width.) The fit likelihood is convoluted with the systematic uncertainty (described below) and integrated to find the 95% confidence level limit on

the number of signal events. The fit is performed twice, with different background functions (an exponential and a sum of two exponentials). Little difference in the fit results is observed, and the result which leads to the more conservative limit is used. All fits report less than a 2.2σ excess.

Efficiencies are measured using the PYTHIA 6.1 [11] Monte Carlo program and a detector simulation. For the masses at the baseline point, $M_{\omega_T} = 210 \text{ GeV}/c^2$ and $M_{\pi_T} = 110 \text{ GeV}/c^2$, we find 44% of generated events contain a photon with $E_T > 25 \text{ GeV}$ and $|\eta| < 1.0$. The efficiency of the photon trigger, fiducial cuts and identification cuts, calibrated with electromagnetic clusters in $Z \rightarrow e^+e^-$ events, is 59%. The efficiency for at least one jet with $E_T > 30 \text{ GeV}$ and $|\eta| < 2.0$ is 91%. The efficiency for one or more tag, calibrated with $b\bar{b}$ data, is 36%. After including the efficiency for the second jet (66%) and the M_{jj} mass window cut (90%), the total $A \cdot \epsilon$ (where A is the acceptance and ϵ is the efficiency) for this choice of masses is 5.1%. The maximum $A \cdot \epsilon$ of approximately 10% is obtained at the largest M_{π_T} and ΔM .

The combined systematic uncertainty of 22% consists of contributions from the uncertainties in photon identification efficiency (14%), tagging efficiency (9%), luminosity measurement (8%), initial-state and final-state radiation (6%), jet energy scale (6%), parton distribution function (5%), and Monte Carlo statistics (4%).

Finally, $A \cdot \epsilon$, the luminosity (85 pb^{-1}), and the upper limit on the number of observed events are combined to yield a limit on $\sigma \cdot B$ (cross section times branching ratio) which can be compared to the theoretical prediction. The model parameters we use are $N_{TC} = 4$ (the number of technicolors, analogous to the three colors in QCD), $Q_D = Q_U - 1 = 1/3$ (the techniquark charges), and $M_T = 100 \text{ GeV}/c^2$ (a dimensionful parameter of order the technicolor interaction scale; cross section scales roughly as M_T^{-2}).

With this parameter set, the $\omega_T \rightarrow \gamma\pi_T$ branching ratio ranges from 35% to 85% in the regions we investigated (the $\pi_T \rightarrow b\bar{b}$ branching ratio is assumed to be 100%). The competing ω_T branching ratios are $q\bar{q}$, $\ell^+\ell^-$ and $\nu\bar{\nu}$. The $Z\pi_T$ and $3\pi_T$ branching ratios have not been calculated and are assumed to be negligible in making the theoretical predictions. We use the CTEQ4L parton distribution function in the Monte Carlo generation. The leading-order theoretical cross section has been scaled up by a K-factor of 1.3, which corrects for higher-order diagrams and is derived by comparing the PYTHIA Monte Carlo Z cross section to the cross section measured in the CDF data. With these model assumptions, combinations of ω_T and π_T mass can be excluded at the 95% confidence level as shown in Figure 2. To define the exclusion region we interpolate between the grid points. The fits to ΔM are sensitive to fluctuations in the data and this causes the ragged exclusion region boundary. For the baseline

point, the model predicts a branching ratio of 63%, and a $\sigma \cdot B$ of 2.32 pb (10.2 events expected). At this point, a $\sigma \cdot B$ of more than 2.38 pb (10.4 events) is excluded at the 95% confidence level.

In conclusion, we have searched for the production of a Technicolor ω_T that decays $\omega_T \rightarrow \gamma\pi_T$ followed by the decay $\pi_T \rightarrow b\bar{b}$ in 85 pb⁻¹ of data collected in the CDF experiment. We observe no evidence of this production and exclude a significant range of ω_T and π_T mass combinations.

We thank the Fermilab staff and the technical staffs of the participating institutions for their vital contributions. We would like to thank K. Lane for useful discussions and J. Womersley for help with the Technicolor Monte Carlo program. This work was supported by the U.S. Department of Energy and National Science Foundation; the Italian Istituto Nazionale di Fisica Nucleare; the Ministry of Education, Science and Culture of Japan; the Natural Sciences and Engineering Research Council of Canada; the National Science Council of the Republic of China; the Swiss National Science Foundation; and the A. P. Sloan Foundation.

- [1] S. Weinberg, Phys. Rev. D **13**, 974 (1976); **19**, 1277 (1979); L. Susskind, Phys. Rev. D **20**, 2619 (1979).
- [2] E. Eichten, K. Lane, and J. Womersley, Phys. Lett. **405B**, 305 (1997); E. Eichten and K. Lane, Phys. Lett. **388B**, 803 (1996).
- [3] F. Abe *et al.*, Nucl. Instrum. Methods Phys. Res., Sect. A **271**, 387 (1988). The z axis points along the proton beam axis; r is the distance from the beamline and θ is the angle from the z axis. Pseudorapidity (η) is $\eta \equiv -\ln(\tan(\theta/2))$ and transverse energy is defined as $E_T = E \sin(\theta)$.
- [4] D. Amidei *et al.*, Nucl. Instrum. Methods Phys. Res., Sect. A **350**, 73 (1994).
- [5] F. Abe *et al.*, Phys. Rev. Lett. **73**, 2662 (1994).
- [6] F. Abe *et al.*, Phys. Rev. D **45**, 1488 (1992).
- [7] F. Abe *et al.*, Phys. Rev. Lett. **74**, 2626 (1995).
- [8] F. Abe *et al.*, Phys. Rev. D **50**, 2966 (1994); F. Abe *et al.*, Phys. Rev. Lett. **73**, 225 (1994).
- [9] In this Letter when two uncertainties are reported, the first is statistical and the second is systematic.
- [10] The $\gamma b\bar{b}$ and $\gamma c\bar{c}$ Monte Carlo programs were provided by M. Mangano. The calculation is leading order based on $q\bar{q}$ and gg initial states and a finite b -quark mass. The Q^2 scale is taken to be the photon E_T squared plus the $b\bar{b}$ or $c\bar{c}$ mass squared. A systematic uncertainty of 30% is found by scaling Q by a factor of two and the quark masses by 10%. An additional 20% systematic uncertainty allows for unmeasured effects.
- [11] H. Bengtsson and T. Sjöstrand, Comput. Phys. Commun. **46**, 43 (1987).

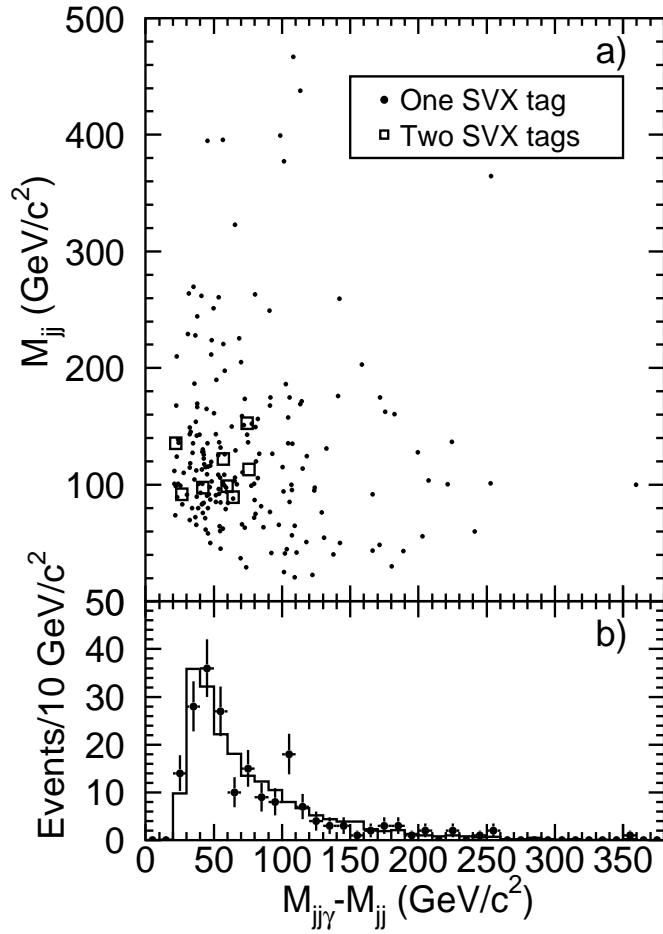


FIG. 1. a) The distribution of M_{jj} plotted *vs* $M_{jj\gamma} - M_{jj}$ for the 200 events with a photon, a tagged jet and a second jet in 85 pb^{-1} of data. b) The projection of the same data in $M_{jj\gamma} - M_{jj}$. The data are represented by the points and the predicted background, normalized to the data, by the histogram. A signal at the baseline model point ($M_{jj} = 110 \text{ GeV}$, $M_{jj\gamma} - M_{jj} = 100 \text{ GeV}$) would have a width of approximately 20 and 5 GeV in these variables respectively.

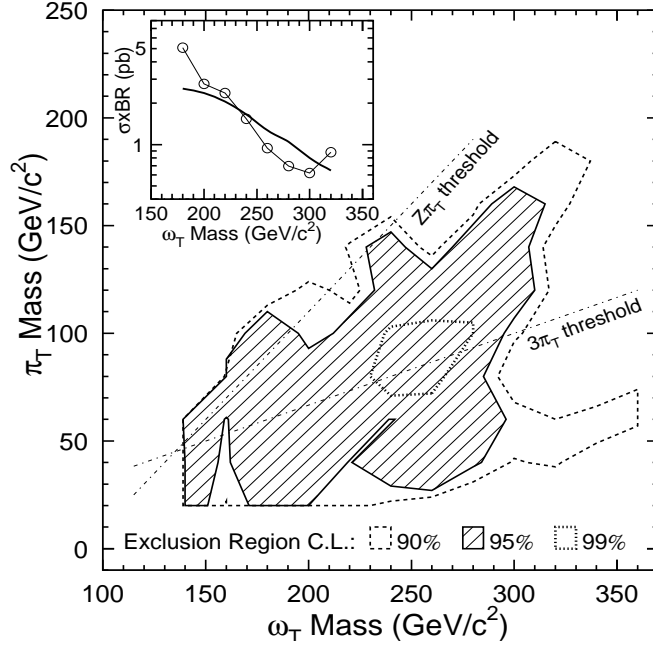


FIG. 2. The 90%, 95% and 99% confidence level exclusion regions in the $M_{\omega_T} - M_{\pi_T}$ mass plane for $\omega_T \rightarrow \gamma\pi_T$ followed by $\pi_T \rightarrow b\bar{b}$. The integrated luminosity of the data sample is 85 pb^{-1} . The difference between the regions is an indication of the robustness of the limits. In the regions below the dash-dotted lines, additional decay modes become available but are assumed to be negligible. The inset shows the limit on $\sigma \cdot B$ for $M_{\pi_T} = 120 \text{ GeV}/c^2$. The circles represent the limit and the solid line represents the theoretical prediction.